25. J. W. Hutchinson, "Singular behavior at the end of tensile crack in a hardening material," J. Mech. Phys. Solids, 16, No. 1 (1968).
26. J. R. Rice and G. F. Rosengren, "Plane strain deformation near a crack tip in a power-law hardening material," J. Mech. Phys. Solids, 16, No. 1 (1968).
27. A. A. Chizhik, "Crack resistance of high-temperature steels and alloys during creep," Fiz. Khim. Mekh. Mater., No. 1 (1986).
28. V. V. Bolotin, "Griffith crack in a damaged viscoelastic medium," Raschety Prochn., Mashinostroenie, No. 26 (1985).
29. L. V. Nikitin, "Application of the Griffith's approach to analysis of rupture in viscoelastic bodies," Int. J. Fract., 24, No. 2 (1984).
30. H. Riedel and J. R. Rice, "Tensile cracks in creeping solids," in: Fracture Mechanics, Am. Soc. Test. Mater. Spec. Tech. Publ., No. 700, Philadelphia (1980).
31. C. Y. Hui and H. Riedel, "The asymptotic stress and strain field near the tip of a growing crack under creep conditions," Int. J. Fract., 17, No. 4 (1981).
32. D. R. Hayhurst, P. R. Brown, and C. J. Morrison, "The role of continuum damage in creep crack growth," Philos. Trans. R. Soc. London, A311 (1984).
33. V. I. Astaf'ev, "Laws of crack growth under creep conditions," Izv. Akad. Nauk SSSR, Mekh. Tverd. Tela, No. 1 (1986).
34. V. I. Astaf'ev, "Description of the fracture process under creep conditions," Izv. Akad. Nauk SSSR, Mekh. Tverd. Tela, No. 4 (1986).
35. L. N. McCartney, "On the energy balance approach to fracture in creeping materials," Int. J. Fract., 19, No. 1 (1982).
36. V. A. Kiselev, "Analysis of crack propagation under creep conditions," Probl. Prochn., No. 4 (1983).
37. G. P. Cherepanov, "Initiation of microcracks and dislocations," Prikl. Mekh., No. 12 (1987).
38. G. P. Cherepanov, "Microcrack growth under monotonic loading," Prikl. Mekh., No. 4 (1988).
39. G. P. Cherepanov, "Closing of microcracks during unloading and the formation of reverse dislocations," Prikl. Mekh., No. 7 (1988).
40. G. P. Cherepanov, "Current problems of fracture mechanics," Probl. Prochn., No. 10 (1987).

NUMERICAL INVESTIGATION OF THE PROCESS OF NONDEFORMABLE CYLINDER PENETRATION AT CONSTANT VELOCITY INTO A COMPRESSIBLE FLUID

S. M. Bakhrakh, O. A. Vinokurov, G. V. Gorbenko, N. P. Kovalev, Yu. A. Osipov, and T. A. Toropova

UDC 531.66

Detailed investigation of the process of nondeformable solid penetration into different media is of great interest in connection with a number of scientific-technical problems of practical importance. Analytical, experimental, and numerical methods (see [1-3, 4-6, 7-10], respectively, say) are utilized to solve the problems occurring here. Because of the complexity of solving the problems by an analytical method, the analysis of a limited number of situations turns out to be accessible. Formulation of experiments in this area is fraught with a number of difficulties. Moreover, the integrated characteristics of the process, for instance, the depth of penetration of the body, are usually fixed in the experiments. A detailed pattern of impactor interaction with deformable compressible media can be obtained by using the numerical solution of similar problems.

The process of bodies of cylindrical shape penetrating a compressible fluid is investigated in this paper by numerical modeling methods. Dependences of the main characteristics of the process (the drag force F, the cavern location relative to the body) on the Mach number $M = V/c_0$ (V is the insertion velocity, and c_0 is the sound speed in the obstacle

Moscow. Translated from Zhurnal Prikladnoi Mekhaniki i Tekhnicheskoi Fiziki, No. 5, pp. 150-155, September-October, 1989. Original article submitted April 27, 1988.

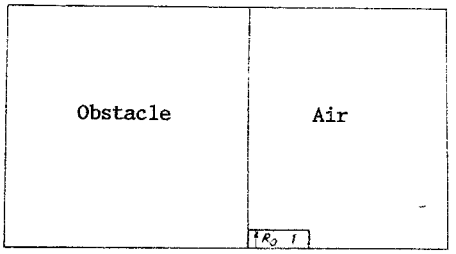

Fig. 1

TABLE 1

Computation number	ρ_0	c_0	V_0	$M=V_0/c_0$	Computation number	ρ_0	c_0	V_0	$M=V_0/c_0$
1	1	2	1	0,5	4	1	0,5	1	2
2	1	1	1	1	5	1	0,25	1	4
3	1	0,5	0,5	1	6	2	1	1	1

material) are obtained for penetration along the normal to the surface.

For high confidence in the results the computations were performed by two different numerical methods included in the set of programs SIGMA [11]. An Euler counting mesh and a fixed body were used in one numerical method; the fluid motion was given relative to the fixed counting mesh.

A regular quadrangular counting mesh whose location remained unchanged relative to the moving cylinder was used in the other method. The crux of this approach is that the counting mesh in the obstacle is shifted together with the penetrating body such that the finitial mutual location of the mesh and the penetrating body is practically conserved throughout the whole computation. Such mesh motion can be assured by giving the shift of each of the mesh points (i, k) according to the law $\tilde{\mathbf{r}}_{ik} = \mathbf{r}_{ik} + (\mathbf{V} - \mathbf{V}_{ik})\Delta t$ ($\mathbf{r}_{ik}$, $\mathbf{V}_{ik}$ are the radius vector and the velocity of the given point).

Computations of such a kind were performed on the basis of the method LÉGAK [12] in which substance concentration and a special algorithm constraining the counting diffusion of the components are relied upon for the numerical modeling of the flows of an inhomogeneous medium (containing several substances). The results of the computations performed by using different numerical methods are in good agreement.

Formulation of the problem at the initial instant (t = 0) is represented in Fig. 1, where the domain 1 is the nondeformable cylindrical impactor of radius R_0 and length d. At the initial time the impactor moves at the velocity V_0. It is assumed that the impactor mass is infinite, i.e., in this case the impactor velocity is constant [$V(t) \equiv V_0$]. The obstacle has the initial density ρ_0, the equation of state is taken in the Mie–Gruneisen form with parameters n = 6, $\Gamma = 0.1$, the coefficient of porosity is K = 1, and the speed of sound c_0 varied. At the initial time the velocity and pressure in the obstacle are zero, and air is a perfect gas with $\gamma = 1.4$. In such a formulation three parameters ρ_0, c_0, V_0 govern the problem.

Numerical parameters of modifications of the problem formulated above are presented in Table 1 (in these computations $R_0 = 1$, d = 3.5, the cylinder length has no value and was selected by starting from convenience in performing the computations).

After collision of the impactor with the deformable obstacle the flow pattern for all modifications of the problem is qualitatively identical and represented in Fig. 2, where the location of the impactor, of the isobar $\bar{p} = 0.01$, of the isochor $\bar{\rho} = 0.98$ is for different times for computation 5 (M = 4), and later the dimensionless time $\tau = tV_0/R_0$, the pressure $\bar{P} = p/(\rho_0 V_0^2)$, and the density $\bar{\rho} = \rho/\rho_0$ are given. It is seen that after the beginning of the collision with the obstacle, the cylinder moves in the cavern such that the insertion drag force F acts only on the cylinder endface for all the times considered (an analogous result was obtained earlier, see [9, 10], say).

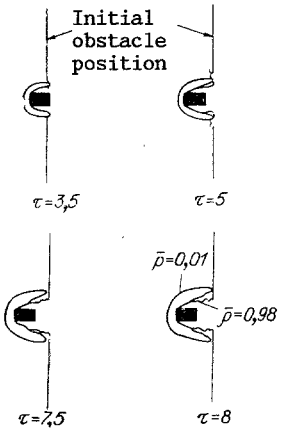

Fig. 2

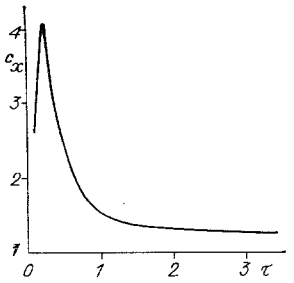

Fig. 3

TABLE 2

c_0	M	D	h	$\bar{p}_{im}$	λ	c_x^{max} (from formula (1))	c_x^{max} (two dimensional computation)
2	0,5	3,7	1,37	3,7	1,7	7,4	—
1	1	2,67	1,6	2,67	1,67	5,34	4,9
0,5	2	2,1	1,91	2,1	1,6	4,2	4,1
0,25	4	1,76	2,32	1,76	1,51	3,52	3,6

TABLE 3

M	c_x (two dimensional computation	c_x (from formula (3))	Difference, %
0,5	1,02	0,98	4
1	1,1	1,09	1
2	1,2	1,24	3
4	1,3	1,32	1,5

The characteristic form of the dependence of the drag force on the time for M = 2 is presented in Fig. 3 ($c_x = 2F/(\rho_0 V_0^2 S)$, $S = \pi R_0^2$ is the area of the cylinder endface). As already noted [9, 10], the insertion process can provisionally be separated into two stages in the time range considered, a nonstationary phase which lasts a brief time after the beginning of the collision and in which the drag force changes abruptly, and a quasistationary stage in which c_x is practically constant.

In the initial time t = 0 the moving cylinder can be considered as a flat piston moving at the velocity V_0. In this case a pressure $p = \rho_0 V_0 D$ acts on the cylinder endface such that

$$c_x^{max} = 2D/V_0 \tag{1}$$

(D is the velocity of shock propagation in the obstacle material). For an equation of state in the Mie–Gruneisen form, the dependence of D on V_0 is described approximately by the relationship $D \approx c_0 + \lambda V_0$, where the function of the parameters of the equation of state is $\lambda = \lambda(n, c_0, \Gamma, \rho_0)$. For the majority of materials λ = 1.4-1.7 [13]. In this case

$$c_x^{max} = (2c_0 + \lambda V_0)/V_0 = 2\lambda + 2/M. \tag{2}$$

The dependence of c_x^{max} on the Mach number is presented in Fig. 4 for λ = 1.5, where the points 1 are the two-dimensional computation and 2 a computation using (2).

The shock adiabatic parameters [13] and values of c_x^{max} obtained from (1) (here V_0 = 1, $h = \rho/\rho_0$, $\bar{p}_{im} = D/V_0$) are presented for different values of c_0 in Table 2 for the equation of state parameters (ρ_0 = 1, n = 6, Γ = 0.1) used in computations performed.

The values of c_x^{max} found in the corresponding two-dimensional computations are sufficiently close to the theoretical values (the maximal difference is less than 10%).

The dependence of c_x on τ ($\tau = tV_0/R_0$) for different M obtained in the two-dimensional computations is displayed in Fig. 5. It is found in the computations that during the time $\tau \approx 1$ the value of c_x drops from its maximum c_x^{max} to a certain value $c_x(M)$ and later practically does not change, the quasistationary insertion stage sets in.

Quasistationary values of c_x are presented in Fig. 6 for the collision of a cylinder with an obstacle for different M {for an incompressible fluid (M = 0), c_x= 0.82 [2]}.

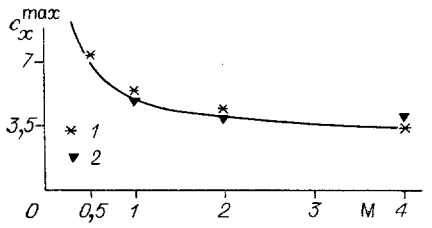

Fig. 4

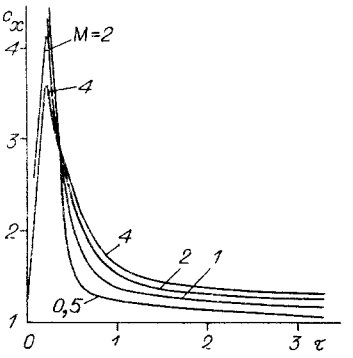

Fig. 5

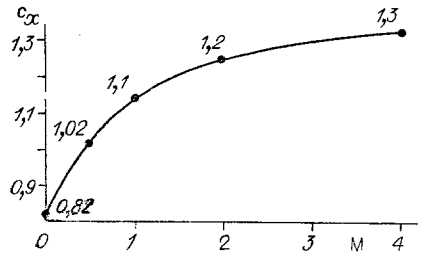

Fig. 6

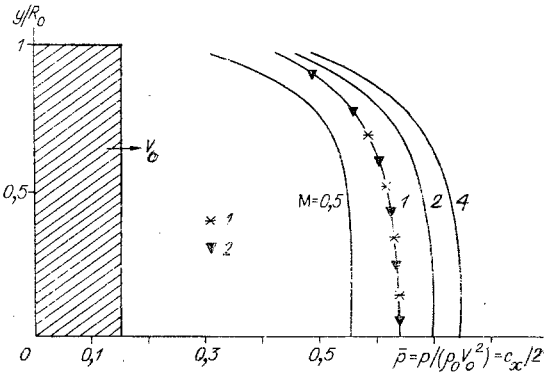

Fig. 7

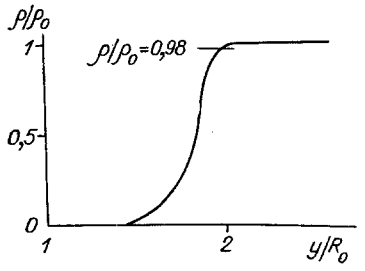

Fig. 8

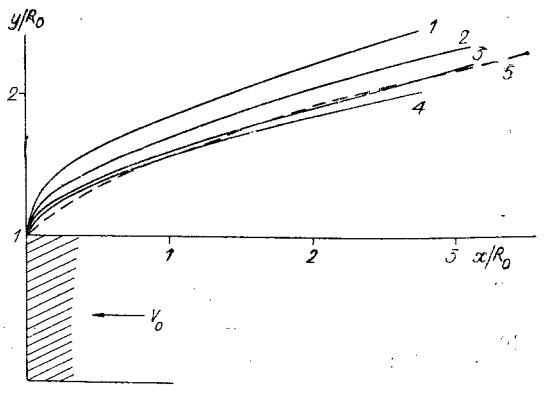

Fig. 9

The dependence of c_x for a cylinder on M, obtained on the basis of the two-dimensional computations is described sufficiently well by the semi-empirical formula

$$c_x = 0.82(1 + M(\lambda - 0{,}5))/(1 + M(\lambda - 1)). \quad (3)$$

This is seen from Table 3 (λ = 1.53). The pressure distribution over the cylinder endface in the quasistationary stage is presented in Fig. 7 for different M, where the points 1 are for M = 1, ρ_0 = 1, c_0 = 0.5, V_0 = 0.5 and the points 2 for M = 1, ρ_0 = 2, c_0 = 1, V_0 = 1.

As already mentioned above the cylinder moves in a cavern after the beginning of the collision, for all the problem modifications considered above. The cavern location relative to the cylinder surface was investigated numerically for different M in the quasistationary motion stage. It must be noted that definite arbitrariness exists in finding the cavern boundary from the two-dimensional computation. For instance, the dependence of the substance density ρ/ρ_0 is given in Fig. 8 as a function of the distance from the cylinder side surface y/R_0 for x/R_0 = 1.6 (M = 1). In principle, any value 1.6-2 can be taken as the cavern boundary at this point depending on what level of ρ/ρ_0 = 0.1-1 is taken as the cavern boundary

criterion. Later we agree to consider the location of the isochor $\rho/\rho_0 = 0.98$ in space as the cavern boundary. The cavern location relative to the cylinder surface in the quasistationary insertion phase is shown in Fig. 9 for M = 0.5, 1, 2, 4, lines 1-4 [the line 5 is a computation using (4)]. It is seen that the higher the M (the higher the insertion velocity V_0 for fixed c_0), the closer does the cavern approach the surface of the cylinder being inserted.

Represented for comparison in Fig. 9 is also the cavern location found in experiments on axisymmetric flow around a disc by an unlimited stream of water for M < 1. The profile for the leading part of the cavern ($x/R_0 < 5$) obtained by processing cavern photographs is presented in [2, p. 118]

$$y/R_0 = (1 + 3x/R_0)^{1/3}. \qquad (4)$$

Taking into account the above about the certain arbitrariness in the selection of the cavern boundary location in two-dimensional computations and the presence generally of the same arbitrariness in the cavern determination when processing the experiment photographs, a deduction can be made about the satisfactory agreement between the theoretical and experimental data on the cavern shape.

LITERATURE CITED

1. M. I. Gurevich, Theory of an Ideal Fluid Jet [in Russian], Izd. Fiz.-Mat. Lit., Moscow (1961).
2. G. V. Logvinovich, Hydrodynamic Flows with Free Boundaries [in Russian], Naukova Dumka, Kiev (1969).
3. A. Ya. Sagomonyan, Penetration [in Russian], Izd. Mosk. Gos. Univ., Moscow (1974).
4. Yu. K. Bivin, V. A. Kolesnikov, and L. M. Flitman, "Determination of mechanical properties of a medium by the method of dynamic insertion," Izv. Akad. Nauk SSSR, Mekh. Tverd. Tela, No. 5 (1982).
5. F. F. Vitman and V. A. Stepanov, "Influence of the strain rate on metal resistance to deformation at 10^2-10^3 m/sec impact velocities," in: Certain Problems of the Strength of Solid Bodies [in Russian], Izd. Akad. Nauk SSSR, Moscow (1959).
6. N. A. Zlatin and G. I. Mishin (eds.), Ballistic Installations and Their Application in Experimental Investigations [in Russian], Nauka, Moscow (1974).
7. V. V. Bashurov and N. A. Skorkin, "Mathematical modeling of axisymmetric body penetration into an obstacle," ChMMSS, 13, No. 2 (1972).
8. A. I. Gulidov, "Penetration of a solid impactor in a deformable obstacle," Tr. 6th All-Union Conf. on Numerical Methods of Solving Elasticity and Plasticity Problems [in Russian], Inst. Teor. Prikl. Mekh., Sib. Otd., Akad. Nauk SSSR, Novosibirsk (1980).
9. V. I. Kondaurov, I. B. Petrov, and A. S. Kholodov, "Numerical modeling of the process of inserting a rigid body of revolution in an elastic-plastic obstacle," Prik. Mekh. Tekh. Fiz., No. 4 (1984).
10. O. M. Belotserkovskii and Yu. M. Davydov, Method of Large Particles in Gasdynamics [in Russian], Nauka, Moscow (1982).
11. M. V. Batalova, S. M. Bakhrakh, O. A. Vinokurov, et al., "SIGMA complex for analysis of two-dimensional gasdynamics problems," Tr. All-Union Seminar on Numerical Methods of Viscous Fluid Mechanics [in Russian], Vychisl. Tsentr, Sib. Otd., Akad. Nauk SSSR, Novosibirsk (1969).
12. S. M. Bakhrakh, V. F. Spiridonov, and A. A. Shanin, "Method of computing gasdynamic flows of an inhomogeneous medium in Lagrange-Euler variables," Dokl. Akad. Nauk SSSR, 276, No. 4 (1984).
13. Ya. B. Zel'dovich and Yu. P. Raizer, Physics of Shocks and High-Temperature Hydrodynamic Phenomena [in Russian], Nauka, Moscow (1966).